Ecotoxicology and Environmental Safety 277 (2024) 116346

Contents lists available at ScienceDirect

Ecotoxicology and Environmental Safety

journal homepage: www.elsevier.com/locate/ecoenv

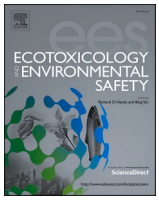

Polyethylene, whose surface has been modified by UV irradiation, induces cytotoxicity: A comparison with microplastics found in beaches

Yudai Ikuno [a], Hirofumi Tsujino [a,b,*], Yuya Haga [a], Sota Manabe [c], Wakaba Idehara [c], Mii Hokaku [c], Haruyasu Asahara [a,d], Kazuma Higashisaka [a,e], Yasuo Tsutsumi [a,d,f,*]

[a] Graduate School of Pharmaceutical Sciences, Osaka University, 1-6 Yamadaoka, Suita, Osaka 565-0871, Japan
[b] Museum Links, Osaka University, 1-13 Machikaneyamacho, Toyonaka, Osaka 560-0043, Japan
[c] School of Pharmaceutical Sciences, Osaka University, 1-6 Yamadaoka, Suita, Osaka 565-0871, Japan
[d] Institute for Open and Transdisciplinary Research Initiatives, 1-1 Yamadaoka, Suita, Osaka 565-0871, Japan
[e] Institute for Advanced Co-Creation Studies, Osaka University, 1-1 Yamadaoka, Suita, Osaka 565-0871, Japan
[f] Global Center for Medical Engineering and Informatics, Osaka University, 2-2 Yamadaoka, Suita, Osaka 565-0871, Japan

ARTICLE INFO

Handling Editor: Richard Handy

Keywords:
Microplastics
Polyethylene
Cytotoxicity
Microplastic degradation
Vacuum ultraviolet irradiation

ABSTRACT

Microplastics, plastic particles 5 mm or less in size, are abundant in the environment; hence, the exposure of humans to microplastics is a great concern. Usually, the surface of microplastics found in the environment has undergone degradation by external factors such as ultraviolet rays and water waves. One of the characteristics of changes caused by surface degradation of microplastics is the introduction of oxygen-containing functional groups. Surface degradation alters the physicochemical properties of plastics, suggesting that the biological effects of environmentally degraded plastics may differ from those of pure plastics. However, the biological effects of plastics introduced with oxygen-containing functional groups through degradation are poorly elucidated owing to the lack of a plastic sample that imitates the degradation state of plastics found in the environment. In this study, we investigated the degradation state of microplastics collected from a beach. Next, we degraded a commercially available polyethylene (PE) particles via vacuum ultraviolet (VUV) irradiation and showed that chemical surface state of PE imitates that of microplastics in the environment. We evaluated the cytotoxic effects of degraded PE samples on immune and epithelial cell lines. We found that VUV irradiation was effective in degrading PE within a short period, and concentration-dependent cytotoxicity was induced by degraded PE in all cell lines. Our results indicate that the cytotoxic effect of PE on different cell types depends on the degree of microplastic degradation, which contributes to our understanding of the effects of PE microplastics on humans.

1. Introduction

Ocean plastic pollution has worsened in recent years. By 2050, it is projected that the amount of plastic waste dumped in the ocean may exceed the number of fish inhabiting it (MacArthur et al., 2016); hence, efforts aimed at plastic waste reduction have increased (Xanthos and Walker, 2017). The negative effects of plastic waste on marine life, such as starvation due to the accidental ingestion of plastic waste, are a cause for concern (Susanti et al., 2020). Among the various types of plastic wastes, much attention has been focused on microplastics, plastic particles 5 mm or less in size (Arthur et al., 2009). The discharge of microplastic-polluted wastewater (e.g., brine) degrades water quality and thus, the water cannot be directly used as potable water (via desalination) or for industrial applications (Panagopoulos and Giannika, 2023, 2022a, 2022b). Microplastics are ubiquitous in the environment, including the ocean (Cole et al., 2011; Kanhai et al., 2017), soil (Büks and Kaupenjohann, 2020), and air (Gasperi et al., 2018; O'Brien et al., 2023). Thus, their impact on living organisms in all ecosystems continues to raise concerns (Besseling et al., 2019); for instance, shellfish (van Cauwenberghe and Janssen, 2014) and fish (Ugwu et al., 2021; Yagi et al., 2022) accidentally swallow microplastics in the ocean, and the presence of these particles have been confirmed in their bodies.

Abbreviations: PS, polystyrene; PE, polyethylene; VUV, vacuum ultraviolet; ATR-IR, attenuated total reflection infrared; FBS, foetal bovine serum; MTT, 3–4,5-dimethyl-thiazol-2-yl-2,5-diphenyl tetrazolium bromide; IC_{50},, 50% inhibitory concentration; CMC, carboxymethyl cellulose sodium salt.

* Corresponding authors at: Graduate School of Pharmaceutical Sciences, Osaka University, 1-6 Yamadaoka, Suita, Osaka 565-0871, Japan.
E-mail addresses: htsujino@phs.osaka-u.ac.jp (H. Tsujino), ytsutsumi@phs.osaka-u.ac.jp (Y. Tsutsumi).

https://doi.org/10.1016/j.ecoenv.2024.116346
Received 4 September 2023; Received in revised form 2 April 2024; Accepted 16 April 2024
Available online 25 April 2024

Moreover, microplastics have been detected in the carcasses of seabirds that had consumed microplastic-contaminated shellfish and fish (Ugwu et al., 2021). Concerns about human consumption of microplastics via the food chain (van Cauwenberghe and Janssen, 2014) have increased as microplastics have been detected in salt (Peixoto et al., 2019; Yang et al., 2015) and drinking water (Eerkes-Medrano et al., 2019; Koelmans et al., 2019). Microplastics have even been detected in human placenta (Ragusa et al., 2021) and blood (Leslie et al., 2022); they may also accumulate in the human body. Human exposure to microplastics increases as microparticles continue to increase in the environment. Therefore, the impact of microplastics on humans should be assessed (Wagner and Reemtsma, 2019).

There are two types of microplastics in the environment: primary and secondary microplastics (Andrady, 2011). Primary microplastics are manufactured as small-sized plastic particles, which are released into the environment through sewage. These are commonly found in toothpaste and cosmetics. Hence, humans are likely to be exposed to microplastics by using these products. In contrast, secondary microplastics have undergone physical and chemical degradation processes facilitated by external factors such as ocean waves and ultraviolet rays to become finer particles. As plastic degrades, its surface is fractured, and functional groups such as carbonyl and hydroxy groups are introduced. Plastics released into the environment are degraded into microplastics of various sizes and shapes (Zhang et al., 2020); thus, microplastics found in the environment are not pure plastics, but plastic particles with altered physical properties and chemical features on the surface. As degraded plastic particles may enter the human body through the consumption of fish and shellfish, the biological effects of degraded microplastics on human health should be evaluated.

Studies have been conducted to evaluate the biological effects of the various sizes and shapes of microplastics. The comparison of the biological effects of 1, 4, and 10 μm polystyrene (PS) revealed that high concentrations of 1 μm PS particles induced cytotoxicity in the human intestinal epithelial cell line Caco-2 (Stock et al., 2019). The evaluation of the *in vitro* uptake of polyethylene (PE), polypropylene, polyethylene terephthalate, and polyvinyl chloride revealed that the cellular uptake of PE was the highest (Stock et al., 2021). Other studies have shown that more inflammatory cytokines are released in the presence of PE fragments than in contact with spherical PE (Choi et al., 2021). However, research focusing on chemical surface modifications associated with plastic degradation is scarce owing to the lack of plastic products that imitate the degradation state of plastics found in the environment. Studies on silica have shown that different surface functional groups have different effects on human embryonic kidney 293 cells (Petushkov et al., 2009). Therefore, it is possible that microplastics with oxygen-containing functional groups, which is one of the characteristics of changes due to surface degradation of microplastics, have a different effect on living organisms than pure microplastics.

Ultraviolet radiations require several years to degrade plastics; hence, simulated sunlight or xenon lamps have been utilized in plastic degradation experiments, and the irradiation time ranges from several days to months (Brandon et al., 2016; Gulmine et al., 2003). However, a plastic degradation method that requires a shorter time is preferable in preparing a sample for evaluating the biological effect of microplastics.

In our previous study, we established a method to easily degrade 24 μm PE and found that degraded PE caused cytotoxicity (Ikuno et al., 2023). In this study, we compared the degraded PE samples we prepared with PE samples collected from the environment, focusing on the chemical state of the surface. The degradation process of plastics is very complex, and it is difficult to completely reproduce the degradation state of microplastics in the environment; so we aimed to mimic microplastics in the environment in terms of introducing oxygen-containing functional groups onto the PE surface. Furthermore, given that microplastics in the order of several hundred μm are often detected in the environment (Lim, 2021) and in human hearts (Yang et al., 2023) and lungs (Jenner et al., 2022), cytotoxicity tests were performed to evaluate its effects on various cell lines using 230 μm PE. The findings of this study are expected to contribute to improvements in microplastic research and help in evaluating the biological risks of microplastic surface degradation.

2. Materials and methods

2.1. Environmental samples measurement

2.1.1. Collection of environmental samples

Sand samples were collected in the presence of these particles high tide line, which contains a large amount of microplastics washed up along the shore and from accumulated dust and other substances of the Onmae and Koshien beaches facing Osaka Bay in Nishinomiya City, Hyogo Prefecture, Japan. The sand samples were sifted to remove large debris and tree branches.

The collected sand samples were then placed in a bucket of water, stirred, and allowed to stand 24 h or longer to separate the microplastics from the sand. PE has a density of 0.919 g/cm^3 and floats on water (density: 1 g/cm^3); therefore, the samples floating on water were collected because they contained PE. Afterwards, the samples were dried and microplastics of approximately 3–5 mm were recovered.

2.1.2. Surface characteristics measurement of environmental samples

Attenuated total reflection infrared (ATR-IR) spectral measurements were performed using an infrared spectrometer (FT/IR-4700) (JASCO Corporation, Tokyo, Japan) equipped with a triglycine sulphate detector. A diamond ATR crystal (angle of incidence: 45°, about 1 reflection) set in a horizontal ATR accessory was used to measure the samples, and all spectra were collected by 32 scans at a resolution of 4 cm^{-1} within the 4000–500 cm^{-1} wavenumber range. First, a background air-blank spectrum without any sample on the ATR crystal was measured. The environmental sample was then placed on the ATR crystal and pressed onto it to record the IR spectrum. The raw spectra are presented as pATR ($= -\log I/I_0$) spectra, where the sample spectral intensity I is divided by the background spectral intensity I_0 before the sample measurement. IR spectra of 18 collected environmental samples were measured.

2.2. Preparation of degraded PE

2.2.1. VUV irradiation treatment of PE

Degraded samples were prepared as described previously (Ikuno et al., 2023) with slight modifications. In brief, FLO-THENE (FG801SN) (Sumitomo Seika Chemicals, Osaka, Japan) with a medium particle size of 80 mesh was used as the PE sample. Degradation experiments were performed using a FLAT EXCIMER EX-mini (Hamamatsu Photonics, Shizuoka, Japan), which irradiates VUV at a wavelength of 172 nm and an irradiation intensity of 65 mW/cm^2 within a range of 86 mm × 40 mm. To degrade the PE sample, approximately 0.2 g of PE sample was spread evenly on the bottom of a Petri dish, approximately 10 mm from the light source, irradiated with VUV for 0.5, 1, and 2 h, and collected in bottles.

2.2.2. Surface characteristics measurement

The ATR-IR spectra of the degraded and undegraded PE samples were recorded using the same method employed for the environmental samples, as described in Section 2.1.2. The surface characteristics of the degraded and ungraded PE samples were compared. In addition, the surface characteristics of the experimentally degraded and environmental PE samples were compared.

2.2.3. Comparison with environmental samples

2.2.3.1. Surface chemical structure. Elemental compositions of the surface were calculated using X-ray photoelectron spectroscopy (XPS: ULVAC-PHI ESCA3057). The XPS parameters included the power of

analysis (wide: 400 W; narrow: 400 W) and monochromatic Al Kα. The survey and high-resolution XPS spectra were collected at fixed analyser pass energies of 93.9 and 29.4 eV, respectively. To confirm the reproducibility, the measurement was performed over three times for each sample. Binding energies were referred to as C−H (sp3) carbon for the C 1 s peak set at 285.0 eV. The peaks were fitted using the PHI MultiPak version 9.2 computer program (ULVAC-PHI Inc.).

2.2.3.2. Surface morphology. Field emission scanning electron microscopy (SU6600) (FE-SEM; Hitachi, Ltd., Tokyo, Japan) was performed to analyse the surface morphology of PE. The experimental or environmental PE samples were fixed on the sample table with carbon tape, and an accelerating voltage of 10 kV was used for measurements.

2.3. Cytotoxicity assessment

2.3.1. Pre-evaluation of PE samples

2.3.1.1. Particle shape. The 1 h degraded and undegraded PE samples used in cytotoxicity tests were transferred to 96-well flat-bottom black plates and imaged using a CellVoyager 8000 (Yokogawa Electric Corporation, Tokyo, Japan). The images were captured using a 4 × magnification dry objective, an LED lamp, and an ORCA®-Flash4.0 CMOS camera (Hamamatsu Photonics, Shizuoka, Japan) with a 525/50 nm bandpass emission filter. The particle shape of the 1 h degraded and undegraded PE samples were compared.

2.3.1.2. Particle size. Particle size distribution was outsourced to Japan Laser Corporation. The device used in this study was HELOS (Sympatec, Clausthal-Zellerfeld, Germany), and a dry air flow dispersion unit RODOS/L(H) (Sympatec, Clausthal-Zellerfeld, Germany) was used as the dispersion unit. Compressed air was used as the dispersion gas, and the dispersion pressure was 2.0 bar. The measurement ranges were R1 (0.1 / 0.18–35 μm) and R5 (0.5 / 4.5–875 μm), and the two ranges were connected by range combination analysis. Moreover, using the volume-based cumulative distribution (Q_3) (%) obtained from the measurements, the volume-based frequency distribution (q_3*) was calculated as follows:

$$q_3^* = dQ_3/\log_{10}(Xu/Xo)$$

Xu represents the upper limit of the particle size in the section, and Xo represents the lower limit. The particle size of the 1 h degraded and undegraded PE samples were compared.

2.3.2. Cell lines and cell culture

The cells selected for the experiment were the immune cell lines RAW264.7 (mouse macrophage cells) and THP-1 (human monocytic leukaemia cells) as well as the epithelial cells A549 (human alveolar adenocarcinoma cells), HaCaT (human keratinocyte cells), and Caco-2 (human intestinal epithelial cells), which are found in the lungs, skin, and intestine, respectively, because they can be exposed to microplastics (Prata et al., 2020). RAW264.7 and THP-1 cells were procured from the American Type Culture Collection (Manassas, VA, USA), A549 and Caco-2 cells were obtained from the RIKEN Cell Bank (Ibaraki, Japan), and HaCaT cells were kindly provided by Dr. Inui of Osaka University, Japan (Inui et al., 1999). RAW264.7, A549, and HaCaT cells were cultured in Dulbecco's Modified Eagle's Medium (high-glucose) (FUJIFILM Wako Pure Chemical Corporation, Osaka, Japan) supplemented with 10% Foetal Bovine Serum (FBS, Biosera, Nuaille, France) and 1% (v/v) penicillin-streptomycin-amphotericin B suspension (Antibiotics; Ab) (FUJIFILM Wako Pure Chemical Corporation, Osaka, Japan). Caco-2 cells were cultured in Eagle's Minimum Essential Medium (FUJIFILM Wako Pure Chemical Corporation, Osaka, Japan) supplemented with 10% FBS and 1% Ab. THP-1 cells were cultured in RPMI-1640 (FUJIFILM Wako Pure Chemical Corporation, Osaka, Japan) containing 10% FBS, 1% Ab, and 0.1% 2-mercaptoethanol (Thermo Fisher Scientific, Waltham, MA, USA). The cells were cultured in 5% CO_2 at 37 °C.

2.3.3. Exposure experiment

The cells were seeded in 96-well plates at a density of 1.5×10^4 (RAW264.7) or 1.0×10^4 (THP-1, A549, HaCaT, and Caco-2) cells per well and allowed to attach for 24 h. The cell culture medium was then replaced by 100 μL of a cell culture medium containing the dispersant 0.001% carboxymethyl cellulose sodium salt (CMC) (FUJIFILM Wako Pure Chemical Corporation, Osaka, Japan) and undegraded or degraded PE samples at different concentrations (0 g/L, 2 g/L, 10 g/L, 25 g/L, 50 g/L, 75 g/L, 100 g/L, 125 g/L, 150 g/L, 175 g/L, and 200 g/L). After 24 h of incubation, cell cytotoxicity was evaluated using 3-(4,5-dimethyl-thiazol-2-yl)-2,5-diphenyl tetrazolium bromide (MTT; Tokyo Chemical Industry, Tokyo, Japan). Measurements were corrected for background signals by subtracting the values from wells incubated without cells and then normalised to the non-treated group as 100%. The MTT assay was performed three times for each cell line and the mean values of cell viability for each concentration were calculated. Finally, the cell viability for each measurement was fitted to a sigmoid curve to calculate the 50% inhibitory concentration (IC_{50}) using Python 3.9.7 software (Python Software Foundation, DE, USA).

We performed annexin V (Bio Legend, San Diego, CA, USA) staining according to the manufacturer's instructions. Briefly, undegraded or degraded PE samples were added to A549 cells at concentrations of 75 and 125 g/L and incubated for 24 h. Staurosporine (200 nM; Cayman CHEMICAL) was used as a positive control. A549 cells were harvested via trypsinization, and 100 μL of cell suspension containing approximately 1×10^5 cells were resuspended in 5 μL of FITC Annexin V at a concentration of 90 μg/mL + 10 μL of propidium iodide (Sigma Aldrich, St. Louis, MO, USA) at a concentration of 1.25 mg/mL, followed by 15 min of incubation at room temperature and protected from light. Then, cells were resuspended with 400 μL of binding buffer (2% FBS, 0.05% sodium azide (Wako)) in phosphate-buffered saline (PBS). Stained cells were analysed via flow cytometry using a MACSQuantX (Miltenyi Biotec, Bergisch Gladbach, Germany).

2.3.4. Morphological observation of cells

A549 cells were seeded in 96-well plates at a density of 1.0×10^4 cells/well and allowed to attach for 24 h. The cell culture medium was then replaced by 100 μL of a cell culture medium containing the dispersant 0.001% CMC, and undegraded or degraded PE samples at 150 g/L concentrations. A group without PE was prepared as a control group. Bright-field imaging was performed using a CellVoyager 8000 every 10 min for 16 h immediately after the PE samples were added. The images were captured using a 60 × water immersion objective, an LED lamp, and an ORCA®-Flash4.0 CMOS camera (Hamamatsu Photonics, Shizuoka, Japan) with a 525/50 nm bandpass emission filter.

2.3.5. Statistical analysis

Results are presented as mean ± SD. Experiments were performed using GraphPad Prism v 9.0, and statistical analyses were performed using two-way analysis of variance (ANOVA) with a Bonferroni multiple comparison test (** $P < 0.01$; **** $P < 0.0001$).

3. Results

3.1. Surface characteristics of PE samples found in the environment

The ATR-IR spectra for the five environmental PE samples out of the 17 collected samples are shown in Fig. 1A–E. Below, the environmental samples shown in Fig. 1A, B, C, D, and E are referred to as Environ. 1, Environ. 2, Environ. 3, Environ. 4, and Environ. 5, respectively. The samples were identified as PE based on the appearance of the C–H stretching bands (2916 cm^{-1} and 2848 cm^{-1}) and C–H bending bands (1465 cm^{-1} and 718 cm^{-1}), both of which are characteristics of this

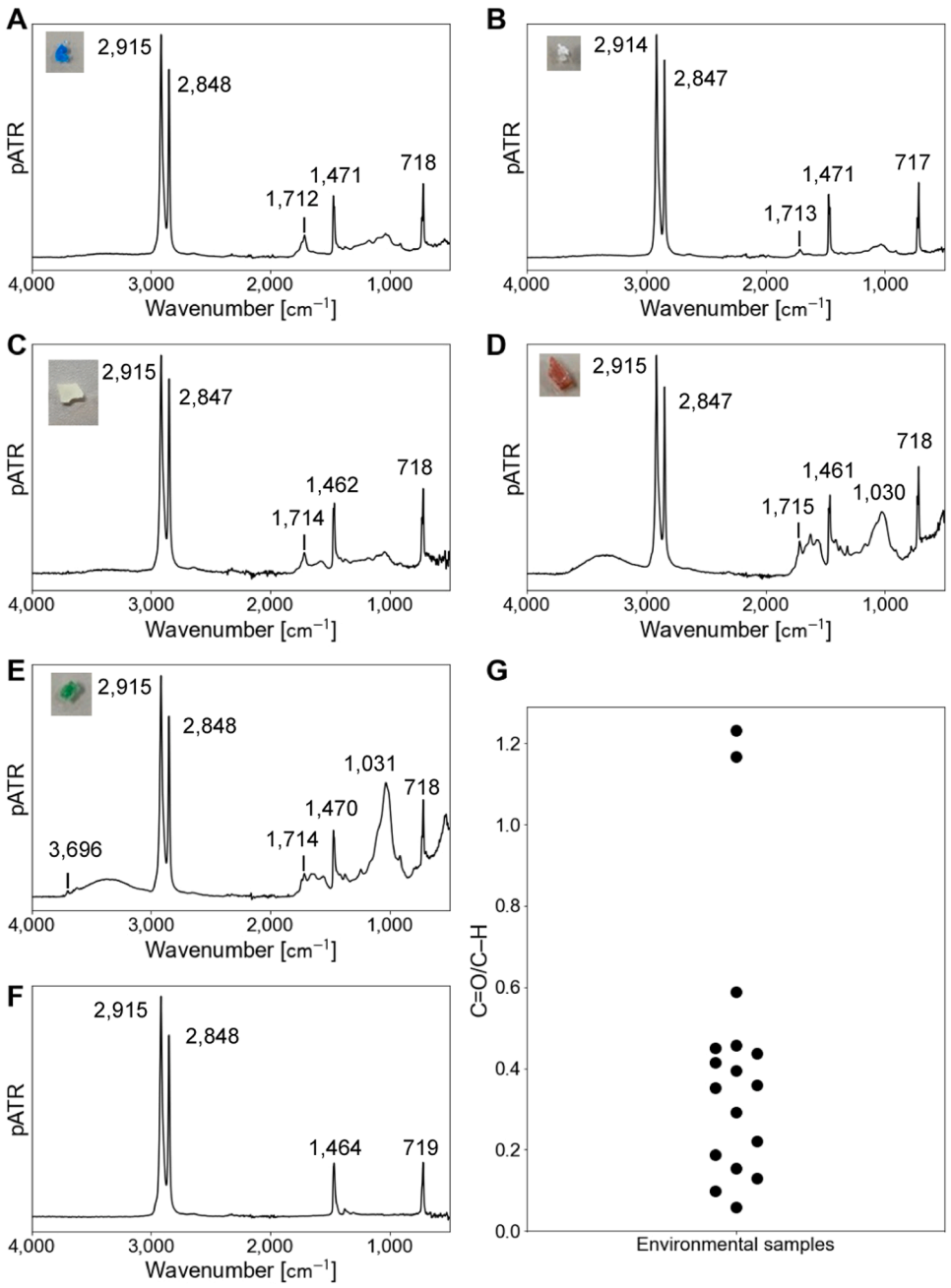

Fig. 1. Raw attenuated total reflectance infrared spectra of (A–E) five typical polyethylene samples collected from the environment and (F) pure polyethylene sample. (G) The degree of degradation (the C═O/C–H ratio) values of 17 environmental samples.

polymer (Fig. 1F). Furthermore, each sample exhibited a band around 1713–1715 cm^{-1}. Environ. 4 and 5 display peaks around 1030 cm^{-1}, indicating the presence of kaolin in these samples. Kaolin is a mineral used as an additive in plastics, and its infrared spectrum exhibits O–H (3697 cm^{-1}) and Si–O stretching bands (1032 cm^{-1}) (Kumar and Lingfa, 2020).

In all samples, an absorption band near 1713–1715 cm^{-1} was detected. These findings suggest the presence of a carbonyl group and indicate the introduction of oxygen-containing functional groups on the surfaces of all environmental samples. Moreover, Environ. 1 and 2, which do not contain kaolin, exhibit an absorption band corresponding to O–H near 1100–1200 cm^{-1}. Furthermore, the ratio of the peak height of C═O (1715 cm^{-1}) to the peak height of C–H (1465 cm^{-1}) (C═O/C–H) was used to determine the degree of degradation. The C═O/C–H ratios were calculated for the 17 environmental samples and shown in Fig. 1G. The C═O/C–H ratios of the Environ. 1, 2, 3, 4, and 5 were 0.36, 0.13, 0.29, 0.41, and 0.35, respectively, thereby suggesting that the degree of degradation varied among the environmental samples. Furthermore, it was found that most of the values of the degree of degradation were between 0.1 and 0.5. Furthermore, all analysed samples exhibited signs of degradation, suggesting that most of the microplastics in the environment have been degraded, either physically or chemically.

3.2. Surface characteristics of experimentally degraded PE particles

The ATR-IR spectra of the PE samples at different exposure intervals during the VUV degradation treatment are shown in Fig. 2. In all spectra, the characteristic absorbance bands around 2915 cm^{-1}, 2848 cm^{-1}, 1465 cm^{-1}, and 720 cm^{-1} corresponded to C–H asymmetric stretching,

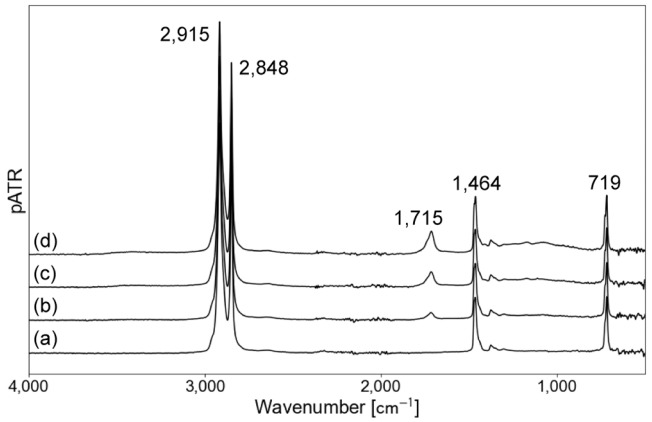

Fig. 2. Raw attenuated total reflectance infrared (pATR = −log I/I_0) spectra of polyethylene samples at different vacuum ultraviolet treatment times: (a) 0 h, (b) 0.5 h, (c) 1 h and (d) 2 h.

C–H symmetric stretching, C–H scissoring bending, and C–H rocking bending respectively. In contrast, the C═O stretching band (1715 cm^{-1}) appeared after the VUV treatment. This change confirms that carbonyl groups were introduced into the PE samples during VUV irradiation, which is a general characteristic of plastic degradation. Furthermore, the ratio of the peak height of C═O (1715 cm^{-1}) to the peak height of C–H (1465 cm^{-1}) (C═O/C–H) was used to determine the degree of deterioration. The C═O/C–H ratio was 0.01 before degradation, 0.14 at 0.5 h, 0.26 at 1 h, and 0.40 at 2 h. The degree of degradation increased with time, and the results indicate that the degree of degradation can be altered by treatment duration. Therefore, the PE samples were successfully degraded by VUV irradiation and oxygen-containing functional groups were introduced on the surface.

The ATR-IR spectra of the experimentally degraded samples were compared with those of the environmental samples shown in Fig. 1A–E. There was no significant difference in the peak positions of the absorption bands derived from the C–H bond of the PE samples at 2916 cm^{-1} and 2848 cm^{-1}; thus, the skeletal structure of the environmental samples and experimentally degraded PE samples did not differ. Furthermore, the peak position of C═O was also around 1713–1715 cm^{-1}, and the value of the degree of deterioration was in the range of 0.1–0.5, which was often present in environmental samples. Therefore, both the experimentally degraded and environmental samples displayed the similar degraded state.

3.3. Comparison of experimentally degraded and environmental PE samples

XPS measurements were performed on Environ. 3, 4, and 5, which maintained their shapes even after ATR-IR measurements, and on the prepared undegraded or degraded PE samples. In the low-resolution XPS spectra, only the C (1 s) peak was observed for undegraded PE, and the C (1 s) peak and O (1 s) peak were observed for the other samples (Fig. 3). Consequently, it was found that the undegraded PE was 100% carbon, and the degraded PE had an increased amount of oxygen (Table 1). The proportion of oxygen in the degraded PE was the same regardless of the degradation time, but the trend was different from the degree of degradation in ATR-IR. This is thought to be due to the difference that ATR-IR measures about 1 μm of the surface, whereas XPS measures several nm of the surface. Therefore, it was suggested that increasing the degraded time may introduce more oxygen atoms into the interior. Additionally, the proportion of oxygen atoms was high in the environmental samples, which is thought to be due to the influence of oxygen atoms contained in additives such as kaolin. Furthermore, due to differences in the molecular weight and crystallinity of PE, it is possible that the amount of oxygen atoms that can be introduced to the PE surface differs. Although there was a difference in oxygen content compared to the environmental sample, it was shown that the prepared degraded sample contained oxygen atoms.

The chemical structure ratios were calculated by separating the C (1 s) peak obtained from the high-resolution XPS spectrum into C–C (284.9 eV), C–N, C–O (286.3 eV), C═O (288.0 eV), and COO (289.0 eV) peaks (Fig. 3B–H, Table 2). As a result, undegraded PE had almost 100% C-C, while degraded PE had an increased proportion of C-O, C═O, and COO. Similar to the atomic composition ratio, the chemical composition ratio was also not found to be dependent on the degradation time. This is thought to be due to the difference in measurement depth between ATR-IR and XPS, and it was suggested that the chemical composition within a few nm of the immediately degraded surface does not change during subsequent degradation in the deep part. Environmental samples also showed an increase in the proportion of chemical compositions containing oxygen atoms compared to undegraded PE. When comparing the chemical composition ratios, no major difference was observed between the experimentally degraded sample and the environmental sample. This suggests that the experimentally prepared degraded PE can reproduce the surface chemical state of PE in the environment in terms of the chemical structure of the PE carbon chain.

SEM images of undegraded and degraded sample and the environmental sample are shown in Fig. 4. The results show that the experimentally degraded samples have a surface morphology similar to that of undegraded PE, regardless of the degraded time. In addition, no fine particles were observed due to degradation. In Environ. 3, shown in Fig. 4E, it was observed that fine particles were embedded on the surface. This is thought to be caused by contact with mineral particles in the environment when the sample is present in the environment. It is possible that this difference is related to the fact that a nitrogen atom was observed in only Environ. 3, but further investigation is required to verify this. In contrast, the influence of fine particles was small in Environ. 4 and 5 (Fig. 4F, G), making it easier to compare with experimentally degraded samples. Many cracks and depressions were observed on the surface of the environmental sample, and the surface unevenness was more complex than that of the experimentally degraded samples. This suggested that experimentally degraded samples could not be reproduced in terms of surface morphology. However, this is not a major problem because the purpose of this study is to create a sample with oxygen-containing functional groups introduced onto the sample surface. Rather, it is important that no change in surface morphology is observed before and after VUV irradiation in order to compare differences in effects between samples with different surface chemical states.

Based on the above results, we achieved our goal of creating a PE sample with a surface chemical state similar to that of microplastics that exist in the environment. Since the degree of degradation of experimentally degraded sample was such that, it could be present in the environment at any degradation time, we selected 1 h degraded sample that had a certain degree of degradation and the degradation time was not too long, and evaluated the differences in the biological effects of undegraded and degraded PE.

3.4. PE degradation experiment and particle size measurement

Microscope observation revealed that there were no significant changes in the particle shape of the 1 h degraded and undegraded PE samples before and after VUV treatment (Fig. 5A, B). The results of the volume-based frequency distribution revealed that the average particle size of the undegraded and 1 h degraded PE samples were 231.4 μm (Figs. 5C) and 231.9 μm (Fig. 5D), respectively, suggesting that average particle size is unaffected by VUV treatment. Moreover, the frequency distribution of the minute particle region (0.1–10 μm) was investigated, as shown in the insets of Fig. 5C and D. There was no significant difference in the particle size of both samples before and after VUV treatment because visible or measurable fine particles were not generated after the VUV treatment.

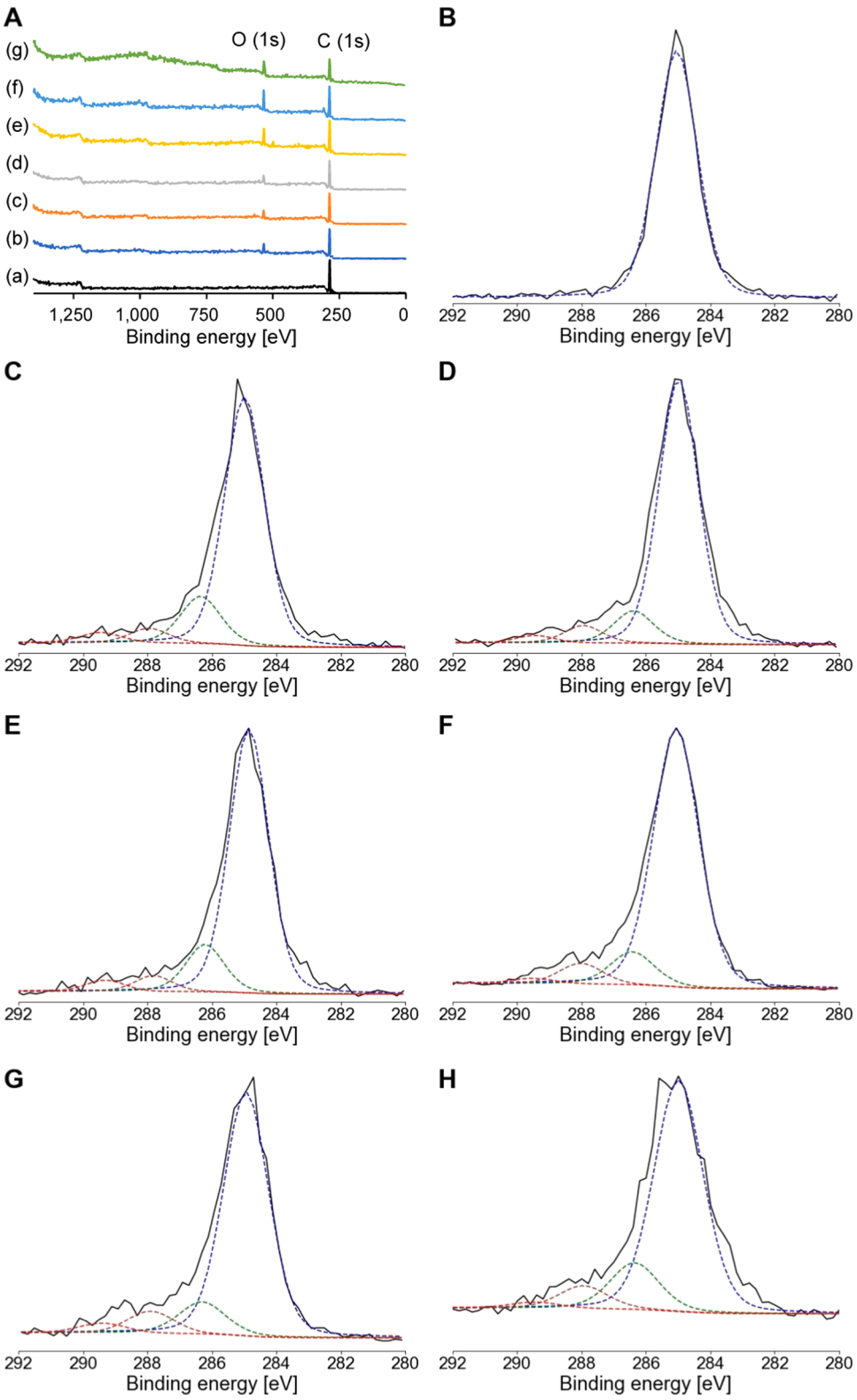

Fig. 3. (A) Low resolution XPS spectra of PE samples (a) without treatment, treated with photo-irradiation for (b) 0.5, (c) 1, (d) 2 h, and (e–g) Environ. 3, 4, 5. High resolution XPS spectra of PE samples (B) without treatment, treated with photo-irradiation for (C) 0.5, (D) 1, (E) 2 h, and (F–H) Environ. 3, 4, 5. Measurement was repeated three times, and representative spectra were shown.

3.5. PE cytotoxicity assessment

The results of the MTT assay revealed that cell viability for all cell lines decreased in the presence of degraded PE (Fig. 6); however, cytotoxicity was not observed in the presence of undegraded PE within the evaluated concentration range.

The IC_{50} was determined to quantitatively evaluate the effects of degraded PE, and the mean ± SD values for three independent

Table 1
Atomic composition ratio of undegraded and degraded samples and environmental samples obtained by XPS. The data show the mean value of technical triplicates.

	Atomic %		
	C1s	N1s	O1s
Undegraded PE	100.0	–	0.0
0.5 h degraded PE	88.6	–	11.4
1 h degraded PE	88.4	–	11.6
2 h degraded PE	88.7	–	11.3
Environ. 3	81.6	1.5	16.9
Environ. 4	81.0	–	19.0
Environ. 5	80.3	–	19.7

Table 2
Chemical composition ratio of undegraded and degraded samples and environmental samples obtained by XPS. The data show the mean value of technical triplicates.

	Chemical Composition Ratio (%)			
	C–C (284.9 eV)	C–N, C–O (286.3 eV)	C═O (288.0 eV)	COO (289.0 eV)
Undegraded PE	99.4	0.2	0.2	0.2
0.5 h degraded PE	79.1	13.8	4.6	2.5
1 h degraded PE	80.8	11.2	5.9	2.2
2 h degraded PE	77.8	13.6	5.6	3.0
Environ. 3	79.2	10.7	6.6	3.5
Environ. 4	80.0	11.8	5.9	2.3
Environ. 5	76.3	15.5	4.6	3.6

experiments are shown in Table 3. The IC_{50} value for THP-1 was the lowest (74.1 ± 10.8 g/L), indicating its susceptibility to degraded PE, whereas A549 exhibited the highest IC_{50} value (119.0 ± 7.2 g/L). Thus, A549 was the least affected by exposure to degraded PE. These results suggest that immune cells are more susceptible than epithelial cells to degraded PE samples because immune cells are highly responsive to foreign substances. The toxicity of PE in different cell lines depends on the presence or absence of polymer degradation.

To investigate how undegraded or degraded PE induces cell death, we evaluated cell death using propidium iodide (PI) and Annexin V staining. PI is a membrane-impermeable fluorescent probe of DNA used as an indicator of necrotic cell death. Annexin V is a surface phosphatidylserine fluorescent probe that localises to the cell surface and detects the early stages of programmed cell death. By flow cytometry analysis, the percentages of PI-positive cells and Annexin V-positive cells in A549 cells exposed to undegraded and degraded PE for 24 h were calculated (Fig. 7). As a result, the percentage of PI and annexin V-positive cells increased in the group to which degraded PE was added, indicating that cell death was being induced. Furthermore, while the proportion of PI-positive and annexin V-negative cells did not increase, the proportion of PI-negative and annexin V-positive cells increased. This suggested that programmed cell death was predominant 24 h after the addition of degraded PE.

3.6. Morphological observation of cells

After the addition of undegraded and degraded PE samples, A549 cells were morphologically observed using time-lapse imaging. There was no change in cell morphology between the undegraded PE group and the control group, to which PE was not added; cell death was not observed in either group (Fig. 8A, B). In contrast, cell death was observed in the group treated with degraded PE (Fig. 8C, D). Within a relatively short period (1–3 h) after the addition of degraded PE, the cells swelled into a round shape, and the cell membrane ruptured, leading to cell death (Fig. 8C). These morphological changes suggest necrosis-like cell death. In contrast, the cells that died 6–8 h after the addition of degraded PE formed protrusions in all directions and eventually died (Fig. 8D). As this characteristic is observed in programmed cell death, exposure of cells to degraded PE may cause programmed cell death. Furthermore, the relatively late occurrence of programmed cell death is consistent with the predominance of programmed cell death 24 h after degraded PE addition. These findings suggest that degraded PE induces cell death through different mechanisms of action.

4. Discussion

All the environmental samples collected in this study were shown to be degraded by ATR-IR measurements (Fig. 1). In this study, samples were taken from a certain beach, so it is possible that these samples were ingested by shellfish living there. Additionally, there is a possibility that it may flow into the sea due to the tides, and if this happens, it may be ingested by marine life. Therefore, consumption of seafood and salt can expose humans to degraded microplastics. Given this, it is extremely important to assess the human health effects of degraded microplastics.

This study showed that oxygen-containing functional groups were introduced on the surface of PE samples within 2 h. ATR-IR measurements confirmed that oxidative functional groups, such as carbonyl groups, were introduced into the degraded PE. The IR spectrum of the degraded PE sample we prepared was similar to the IR spectrum of the PE samples collected from the environment. XPS analysis confirmed that the chemical composition ratios of the experimentally degraded samples were similar to those of the environmental samples. SEM observation showed that the surface morphology of the experimentally degraded samples was simpler than that of the environmental samples. Therefore, further study is required to reproduce the surface morphology. However, the experimentally degraded PE had a similar surface morphology to the undegraded PE. Furthermore, microscopic observations and particle size distribution measurements confirmed that the PE particles did not change in shape or size after degradation. Although it was not possible to completely simulate the complex deterioration state of microplastics in the environment, we were able to create a sample similar to the environmental sample in that it had oxygen-containing functional groups on the sample surface.

By performing cytotoxicity tests, we evaluated the biological effects of PE samples on different cell lines. It was revealed that only degraded PE induced cytotoxicity (Fig. 6), and cytotoxicity was not affected by the particle size of the samples. The main difference between the degraded and undegraded PE samples was the chemical state of the PE surface, as revealed by the IR (Fig. 2) and the XPS results (Table 2); therefore, the cytotoxic effects of PE could be due to the hydrophilic hydroxyl and carbonyl groups introduced on the surface of the PE samples. Moreover, these groups enhanced the hydrophilicity of the degraded PE compared with the hydrophobic undegraded polymer; therefore, the dispersion of the degraded PE into the medium increased, enabling contact between PE and the cells. However, the addition of CMC to the test medium may have also aided in the dispersion of undegraded PE although the dispersion effect was lower than that observed for the degraded PE samples. Nevertheless, the effect of dispersibility was considered less important because the undegraded PE sample did not induce cytotoxicity, even at high concentrations.

Furthermore, changes in the chemical state of the PE surface may affect the cell membranes upon contact with cells (de de de Souza Machado et al., 2018). Because the surface of the phospholipid bilayer in the cell membrane is hydrophilic, the influence of the hydrophobic undegraded PE samples decreased. Moreover, it is possible that the introduction of hydrophilic groups to the PE surface may improve its affinity towards the cell membrane and induce cell damage; this reaction may explain why the degraded PE sample induced cytotoxicity. Carboxyl group–modified silica particles have been shown to damage

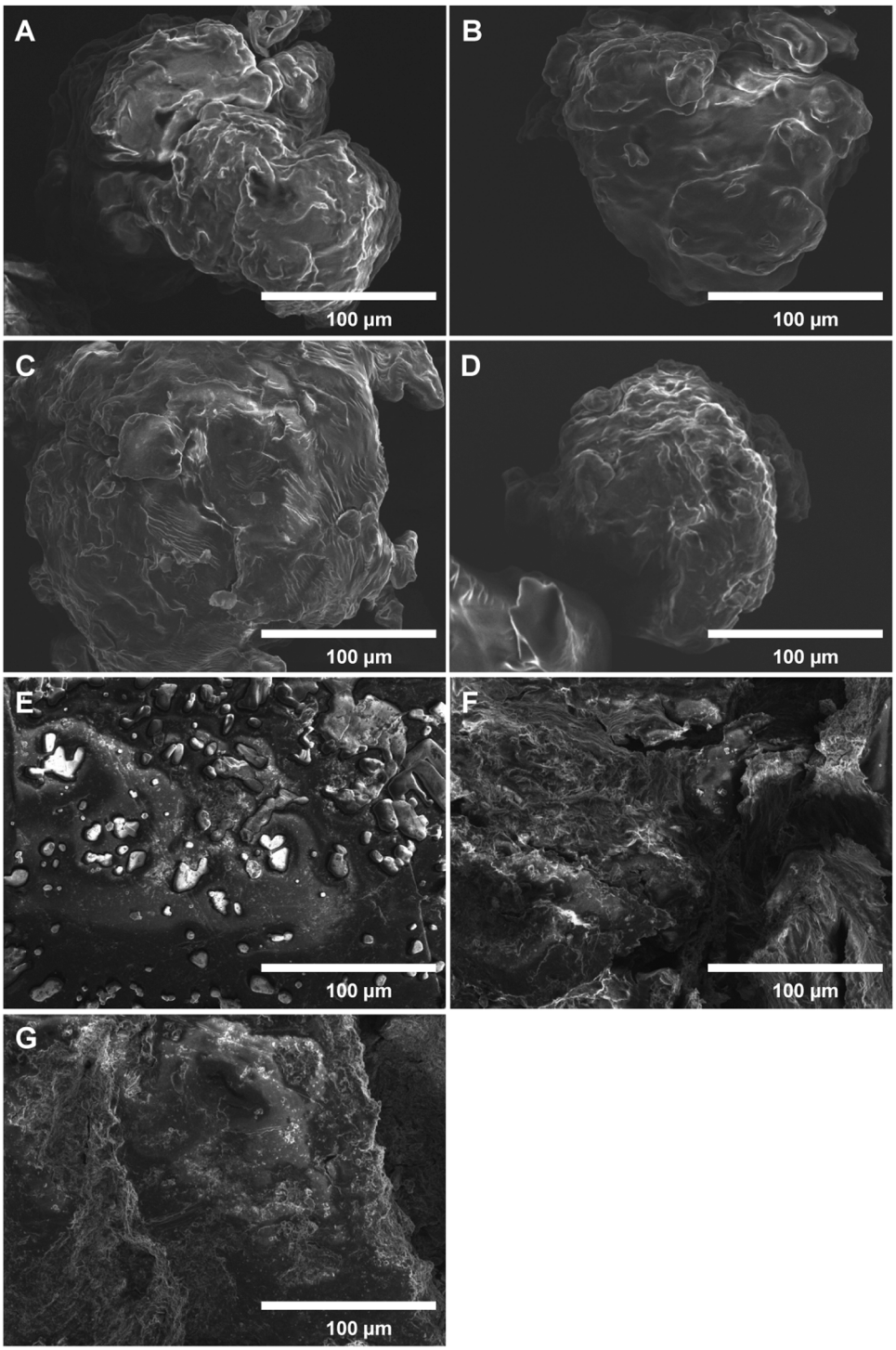

Fig. 4. SEM images of PE samples (A) without treatment, treated with photo-irradiation for (B) 0.5, (C) 1, (D) 2 h, and (E–G) Environ. 3, 4, 5.

cell membranes (Petushkov et al., 2009). Microscopic observation revealed that the cell membrane of the cells was damaged (Fig. 8C, D). In particular, the cell death that occurred 1–3 h after the addition of degraded PE is considered necrosis-like cell death due to physical damage to the cells, and degraded PE was thought to have directly damaged the cell membrane. Moreover, particle size distribution measurements (Fig. 5C, D) confirmed the presence of PE fragments ≤ 1 μm in size, which can be directly taken up by cells (Mao et al., 2013). Hence, it is possible that small-sized PE particles were taken up by the cells; however, only degraded PE induced an adverse effect when taken up by the cells. The apoptosis-like cell death that occurred 6–8 h after the addition of degraded PE was thought to be due to the cellular uptake of degraded PE. Indeed, Annexin V assay showed increased apoptosis rate in cells treated with degraded PE for 24 h. In the future, it will be necessary to elucidate the mechanism of cell death in more detail by evaluating differences in cellular uptake ability and the effects on intracellular lysosomes and mitochondria.

In addition, the concentration of PE used in the experiments was higher than the actual exposure of humans to microplastics. According to a study that detected microplastics in blood, the maximum PE concentration in blood was 7.1 μg/mL (Leslie et al., 2022), which is much lower than the concentration at which cytotoxicity was observed in this

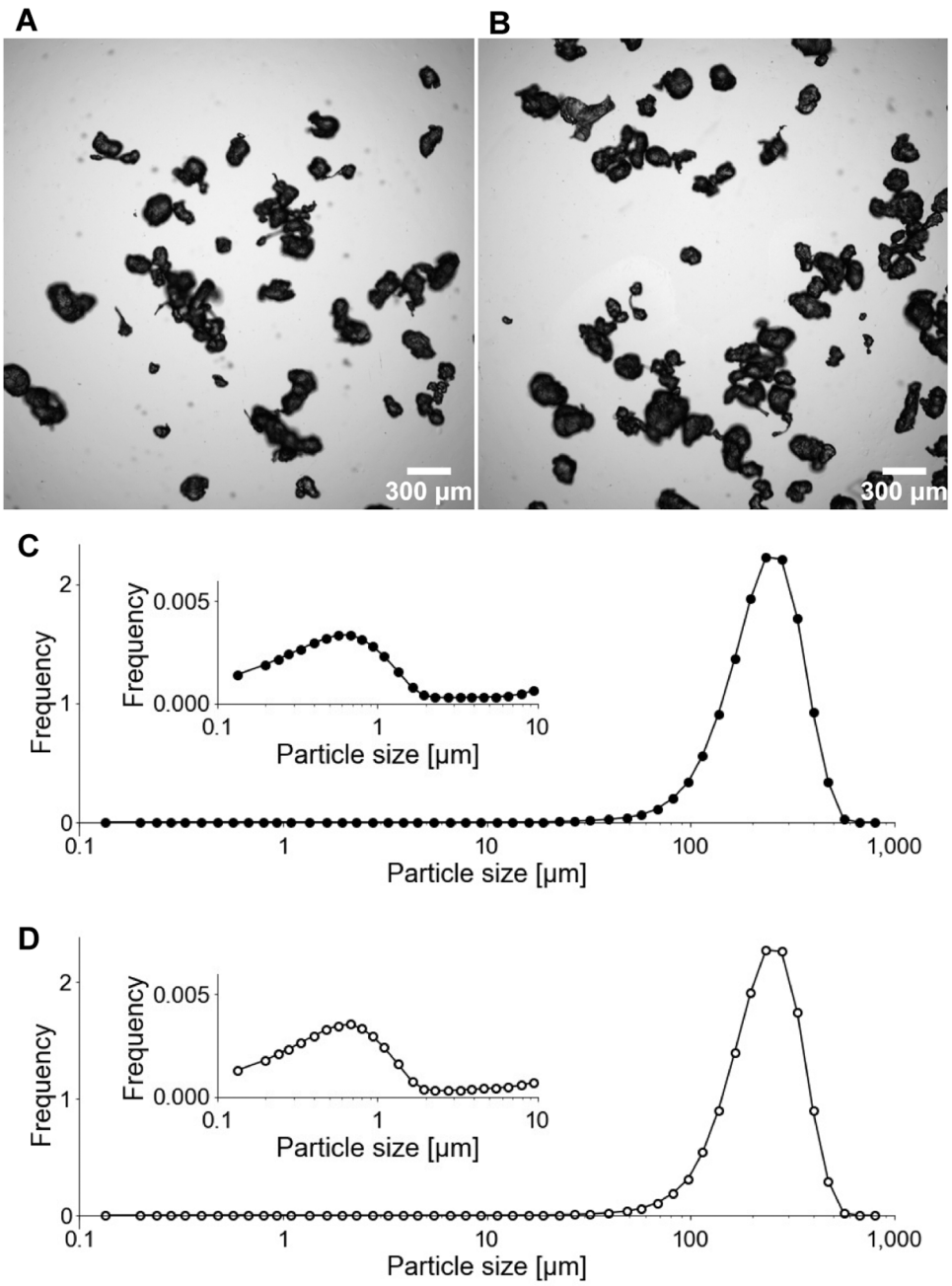

Fig. 5. Particle size distribution of polyethylene (PE) samples and corresponding microscopic images of (A) undegraded and (B) 1 h degraded PE. Scale bars: 300 μm. Volume-based frequency distribution of (C) undegraded and (D) 1 h degraded PE. The measuring range was 0.1–875 μm. Measurements were repeated three times and average values are shown. Inset shows an enlarged view of minute particle region (0.1–10 μm) in each figure.

study. However, several unknown factors remain, such as the accumulation of microplastics in organs. Therefore, a detailed kinetic analysis is required. In addition, because PE has low density and floats in the medium, it is possible that the number of PE particles acting on the cells is much lower than their concentration. Because PE is floating during culture, it is possible that PE came into contact with the cells only at the moment of PE addition. Nevertheless, as cytotoxicity was observed with degraded PE, it is possible that even slight contact with PE may affect cells. Microplastics that have migrated to tissues and organs are thought to be in contact with cells, so even a small concentration or number of particles can have a negative impact on those areas. Additionally, it is generally believed that the effect of fine particles becomes greater as the size decreases (Sharma et al., 2023), and degraded PE of smaller size may have an effect at lower concentrations. Moreover, the cytotoxicity test used in this study only evaluated the ability of a substance to induce cell death. Therefore, future research should focus on evaluating other cytotoxic effects of degraded PE on cells, such as inflammatory cytokine production.

Since PE floats in the medium, indirect rather than direct effect of PE might cause cell death. It is known that monocarboxylic and dicarboxylic acids are generated as PE degrades (Rummel et al., 2022), so it is possible that these elution into the medium may have had an adverse effect on the cells. Therefore, further experiments are needed to consider the buoyancy of PE and elution from degraded PE.

In this study, a large-size environmental sample was collected for the convenience of ATR-IR measurements; however, micro- and nano-sized microplastics exist in the environment (Zhang et al., 2020). Because collecting small microplastics is difficult, assessing their cytotoxicity and

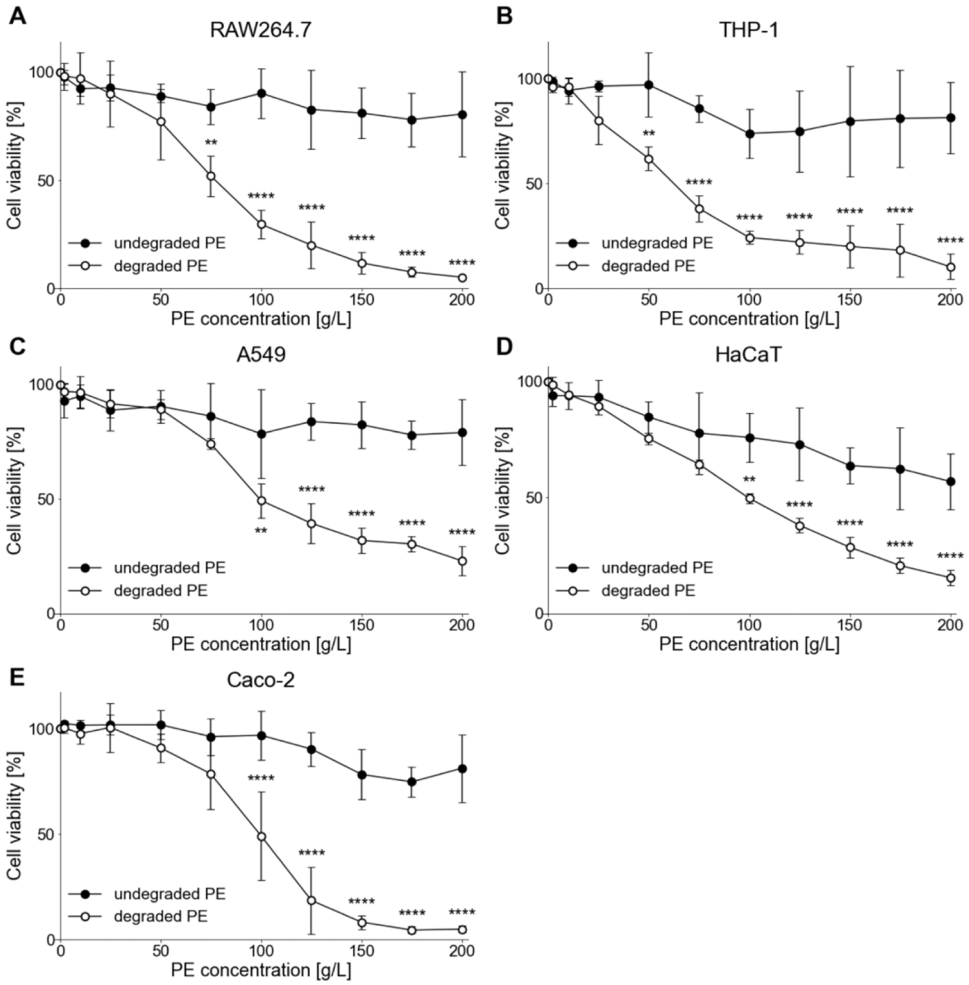

Fig. 6. Cell viability curves obtained through the MTT assay (n = 3, mean ± SD). (A) RAW264.7, (B) THP-1, (C) A549, (D) HaCaT, and (E) Caco-2 cell lines. Significance was assessed using two-way ANOVA followed by Bonferroni multiple comparison test as follows: ** $P < 0.01$; **** $P < 0.0001$.

Table 3
IC_{50} for undegraded and degraded PE samples. Mean values (n = 3, ± SD) for the independent experiments are included.

Cell line	IC_{50} [g/L]	
	undegraded PE	degraded PE
RAW264.7	≥ 200	80.5 ± 8.0
THP-1	≥ 200	74.1 ± 10.8
A549	≥ 200	119.0 ± 7.2
HaCaT	≥ 200	107.3 ± 3.3
Caco-2	≥ 200	98.6 ± 15.9

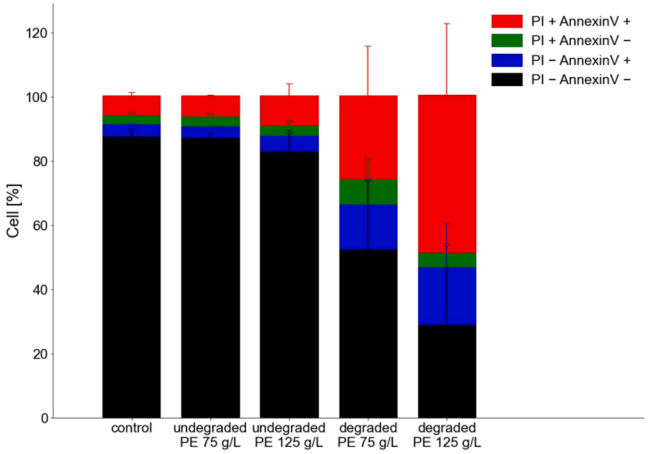

Fig. 7. Percentage of PI and Annexin V positive cells obtained by flow cytometry (n = 3, mean ± SD).

performing other related investigations also prove difficult. Even if small-sized microplastics are recovered' from the environment, it is difficult to classify their physical properties, such as shape and type. Therefore, it is especially important to further develop the samples used in this study and create standard products that better reproduce the degradation state of microplastics in the environment. In the future, it is expected that a technique for collecting micro- and nano-sized microplastics and measuring their surface properties will be established.

5. Conclusions

In this study, we evaluated cytotoxic effects on immune and epithelial cells using VUV-irradiated PE samples. VUV-irradiated PE samples were compared with microplastics from the environment and were suggested to be similar to environmental samples in that oxygen-containing functional groups were introduced on the surface. We also found that degraded PE induced necrosis-like cell death in immune and epithelial cells. One major finding of this study is that the cytotoxicity of PE increased due to surface degradation. Evaluations using plain microplastics that have been performed so far may have underestimated

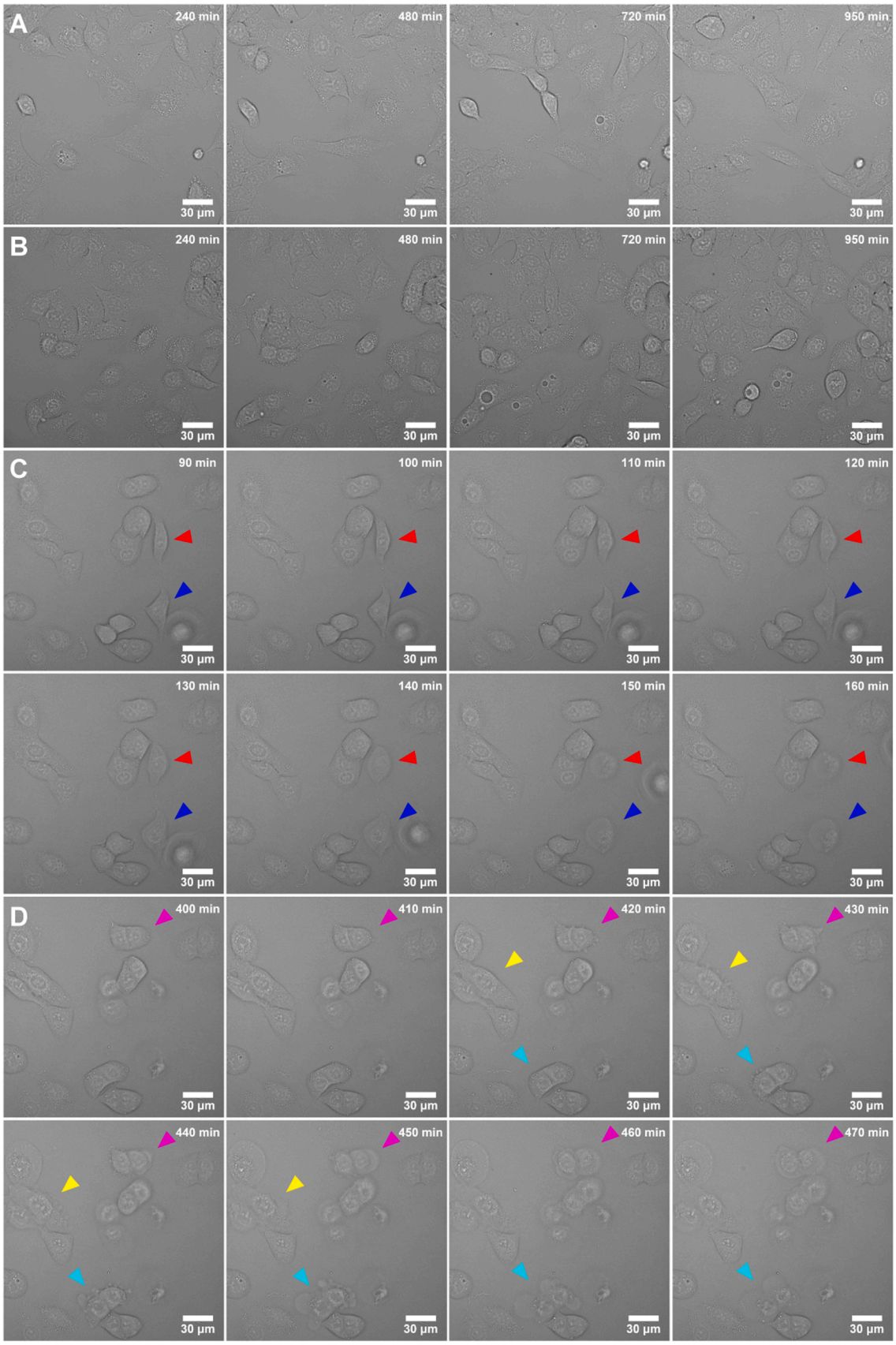

Fig. 8. Bright-field images of the (A) control group at 240, 480, 720, and 950 min, (B) group treated with 150 g/L undegraded PE at 240, 480, 720, and 950 min and (C) group treated with 150 g/L degraded PE at 90–160 min and (D) 400–470 min. Images were taken every 10 min for 16 h. Scale bars: 30 μm. Arrowheads indicate dead cells.

the results. In the future, it is necessary to conduct various biological impact assessments focusing on degraded state and evaluate the effects of degraded microplastics. To this end, it is desirable to develop standard products that better reproduce the deterioration state of microplastics in the environment. Therefore, the degradation experiments performed in this study are considered to be an effective method to chemically modify the surface of PE, and are a versatile method that can be applied to particles of various sizes and other microplastic particles such as polystyrene. Our study can help advance research on the characteristics, particle size, degree of degradation, and biological effects of microplastics on various organisms.

Funding

This work was supported by Japan Science and Technology Agency (Grant Number JPMJSP2138), Japan Society for the Promotion of Science (Grant Number JP21387863), and Ministry of Health Labour and Welfare (Grant Number JPMH21447937), and The Sumitomo Foundation for Environmental Research Projects.

CRediT authorship contribution statement

Haruyasu Asahara: Methodology. **Kazuma Higashisaka:** Methodology. **Yasuo Tsutsumi:** Supervision, Project administration. **Yudai Ikuno:** Writing – original draft, Visualization, Methodology, Investigation, Data curation. **Hirofumi Tsujino:** Project administration, Conceptualization. **Yuya Haga:** Project administration, Methodology. **Sota Manabe:** Methodology, Investigation. **Wakaba Idehara:** Methodology, Investigation. **Mii Hokaku:** Methodology, Investigation.

Declaration of Generative AI and AI-assisted technologies in the writing process

None.

Declaration of Competing Interest

The authors declare the following financial interests/personal relationships which may be considered as potential competing interests: Yudai Ikuno reports financial support was provided by Japan Science and Technology Agency. Yasuo Tsutsumi reports was provided by Japan Society for the Promotion of Science. Hirofumi Tsujino reports financial support was provided by Ministry of Health Labour and Welfare. Yasuo Tsutsumi reports financial support was provided by The Sumitomo Foundation for Environmental Research Projects.

Data availability

Data will be made available on request.

Acknowledgements

The authors would like to express their gratitude to Dr. Kei Ohkubo and Dr. Yuki Itabashi of the Institute for Open and Transdisciplinary Research Initiatives, Osaka University, Osaka, Japan, for providing us the opportunity to use the FLAT EXCIMER EX-mini. This research was partially supported by the Research Support Project for Life Science and Drug Discovery (Basis for Supporting Innovative Drug Discovery and Life Science Research) from AMED under Grant Number JP23ama121054.

References

Andrady, A.L., 2011. Microplastics in the marine environment. Mar. Pollut. Bull. 62, 1596–1605. https://doi.org/10.1016/j.marpolbul.2011.05.030.

Arthur, C., J. Baker and H. Bamford (eds). 2009. Proceedings of the International Research Workshop on the Occurrence, Effects and Fate of Microplastic Marine Debris. Sept 9-11, 2008. NOAA Technical Memorandum NOS-OR&R-30.

Besseling, E., Redondo-Hasselerharm, P., Foekema, E.M., Koelmans, A.A., 2019. Quantifying ecological risks of aquatic micro- and nanoplastic. Crit. Rev. Environ. Sci. Technol. 49, 32–80. https://doi.org/10.1080/10643389.2018.1531688.

Brandon, J., Goldstein, M., Ohman, M.D., 2016. Long-term aging and degradation of microplastic particles: comparing in situ oceanic and experimental weathering patterns. Mar. Pollut. Bull. 110, 299–308. https://doi.org/10.1016/j.marpolbul.2016.06.048.

Büks, F., Kaupenjohann, M., 2020. Global concentrations of microplastics in soils – a review. SOIL 6, 649–662. https://doi.org/10.5194/soil-6-649-2020.

van Cauwenberghe, L., Janssen, C.R., 2014. Microplastics in bivalves cultured for human consumption. Environ. Pollut. 193, 65–70. https://doi.org/10.1016/j.envpol.2014.06.010.

Choi, D., Hwang, J., Bang, J., Han, S., Kim, T., Oh, Y., Hwang, Y., Choi, J., Hong, J., 2021. In vitro toxicity from a physical perspective of polyethylene microplastics based on statistical curvature change analysis. Sci. Total. Environ. 752, 142242 https://doi.org/10.1016/j.scitotenv.2020.142242.

Cole, M., Lindeque, P., Halsband, C., Galloway, T.S., 2011. Microplastics as contaminants in the marine environment: a review. Mar. Pollut. Bull. 62, 2588–2597. https://doi.org/10.1016/j.marpolbul.2011.09.025.

Eerkes-Medrano, D., Leslie, H.A., Quinn, B., 2019. Microplastics in drinking water: a review and assessment. Curr. Opin. Environ. Sci. Health 7, 69–75. https://doi.org/10.1016/j.coesh.2018.12.001.

Gasperi, J., Wright, S.L., Dris, R., Collard, F., Mandin, C., Guerrouache, M., Langlois, V., Kelly, F.J., Tassin, B., 2018. Microplastics in air: are we breathing it in? Curr. Opin. Environ. Sci. Health 1, 1–5. https://doi.org/10.1016/j.coesh.2017.10.002.

Gulmine, J.V., Janissek, P.R., Heise, H.M., Akcelrud, L., 2003. Degradation profile of polyethylene after artificial accelerated weathering. Polym. Degrad. Stab. 79, 385–397. https://doi.org/10.1016/S0141-3910(02)00338-5.

Ikuno, Y., Tsujino, H., Haga, Y., Asahara, H., Higashisaka, K., Tsutsumi, Y., 2023. Impact of degradation of polyethylene particles on their cytotoxicity. Microplastics 2, 192–201. https://doi.org/10.3390/microplastics2020015.

Inui, S., Lee, Y.F., Haake, A.R., Goldsmith, L.A., Chang, C., 1999. Induction of TR4 orphan receptor by retinoic acid in human HaCaT keratinocytes. J. Invest. Dermatol. 112, 426–431. https://doi.org/10.1046/j.1523-1747.1999.00548.x.

Jenner, L.C., Rotchell, J.M., Bennett, R.T., Cowen, M., Tentzeris, V., Sadofsky, L.R., 2022. Detection of microplastics in human lung tissue using μFTIR spectroscopy. Sci. Total. Environ. 831, 154907 https://doi.org/10.1016/j.scitotenv.2022.154907.

Kanhai, L.D.K., Officer, R., Lyashevska, O., Thompson, R.C., O'Connor, I., 2017. Microplastic abundance, distribution and composition along a latitudinal gradient in the Atlantic Ocean. Mar. Pollut. Bull. 115, 307–314. https://doi.org/10.1016/j.marpolbul.2016.12.025.

Koelmans, A.A., Mohamed Nor, N.H., Hermsen, E., Kooi, M., Mintenig, S.M., de France, J., 2019. Microplastics in freshwaters and drinking water: critical review and assessment of data quality. Water Res. 155, 410–422. https://doi.org/10.1016/j.watres.2019.02.054.

Kumar, A., Lingfa, P., 2020. Sodium bentonite and kaolin clays: comparative study on their FT-IR, XRF, and XRD. Mater. Today Proc. 22, 737–742. https://doi.org/10.1016/j.matpr.2019.10.037.

Leslie, H.A., van Velzen, M.J.M., Brandsma, S.H., Vethaak, A.D., Garcia-Vallejo, J.J., Lamoree, M.H., 2022. Discovery and quantification of plastic particle pollution in human blood. Environ. Int. 163, 107199 https://doi.org/10.1016/j.envint.2022.107199.

Lim, X., 2021. Microplastics are everywhere — but are they harmful? Nature 593, 22–25. https://doi.org/10.1038/d41586-021-01143-3.

Dame Ellen MacArthur, Dominic Waughray, Martin R. Stuchtey, 2016. The New Plastics Economy: Rethinking the future of plastics.

Mao, Z., Zhou, X., Gao, C., 2013. Influence of structure and properties of colloidal biomaterials on cellular uptake and cell functions. Biomater. Sci. 1, 896–911. https://doi.org/10.1039/c3bm00137g.

O'Brien, S., Rauert, C., Ribeiro, F., Okoffo, E.D., Burrows, S.D., O'Brien, J.W., Wang, X., Wright, S.L., Thomas, K.V., 2023. There's something in the air: a review of sources, prevalence and behaviour of microplastics in the atmosphere. Sci. Total. Environ. 874, 162193 https://doi.org/10.1016/j.scitotenv.2023.162193.

Panagopoulos, A., Giannika, V., 2022a. Decarbonized and circular brine management/valorization for water & valuable resource recovery via minimal/zero liquid discharge (MLD/ZLD) strategies. J. Environ. Manag. 324, 116239 https://doi.org/10.1016/j.jenvman.2022.116239.

Panagopoulos, A., Giannika, V., 2022b. Comparative techno-economic and environmental analysis of minimal liquid discharge (MLD) and zero liquid discharge (ZLD) desalination systems for seawater brine treatment and valorization. Sustain. Energy Technol. Assess. 53, 102477 https://doi.org/10.1016/j.seta.2022.102477.

Panagopoulos, A., Giannika, V., 2023. Study on the water resources and the opportunities for sustainable desalination & minimal/zero liquid discharge (MLD/ZLD) practices in Greece (Eastern Mediterranean). Sustain. Water Resour. Manag. 9, 106. https://doi.org/10.1007/s40899-023-00884-5.

Peixoto, D., Pinheiro, C., Amorim, J., Oliva-Teles, L., Guilhermino, L., Vieira, M.N., 2019. Microplastic pollution in commercial salt for human consumption: a review. Estuar. Coast Shelf Sci. 219, 161–168. https://doi.org/10.1016/j.ecss.2019.02.018.

Petushkov, A., Intra, J., Graham, J.B., Larsen, S.C., Salem, A.K., 2009. Effect of crystal size and surface functionalization on the cytotoxicity of silicalite-1 Nanoparticles. Chem. Res. Toxicol. 22, 1359–1368. https://doi.org/10.1021/tx900153k.

Prata, J.C., da Costa, J.P., Lopes, I., Duarte, A.C., Rocha-Santos, T., 2020. Environmental exposure to microplastics: an overview on possible human health effects. Sci. Total. Environ. 702, 134455 https://doi.org/10.1016/j.scitotenv.2019.134455.

Ragusa, A., Svelato, A., Santacroce, C., Catalano, P., Notarstefano, V., Carnevali, O., Papa, F., Rongioletti, M.C.A., Baiocco, F., Draghi, S., D'Amore, E., Rinaldo, D., Matta, M., Giorgini, E., 2021. Plasticenta: first evidence of microplastics in human placenta. Environ. Int. 146, 106274 https://doi.org/10.1016/j.envint.2020.106274.

Rummel, C.D., Schäfer, H., Jahnke, A., Arp, H.P.H., Schmitt-Jansen, M., 2022. Effects of leachates from UV-weathered microplastic on the microalgae Scenedesmus vacuolatus. Anal. Bioanal. Chem. 414, 1469–1479. https://doi.org/10.1007/s00216-021-03798-3.

Sharma, V.K., Ma, X., Lichtfouse, E., Robert, D., 2023. Nanoplastics are potentially more dangerous than microplastics. Environ. Chem. Lett. 21, 1933–1936. https://doi.org/10.1007/s10311-022-01539-1.

de Souza Machado, A.A., Kloas, W., Zarfl, C., Hempel, S., Rillig, M.C., 2018. Microplastics as an emerging threat to terrestrial ecosystems. Glob. Chang. Biol. 24, 1405–1416. https://doi.org/10.1111/gcb.14020.

Stock, V., Böhmert, L., Lisicki, E., Block, R., Cara-Carmona, J., Pack, L.K., Selb, R., Lichtenstein, D., Voss, L., Henderson, C.J., Zabinsky, E., Sieg, H., Braeuning, A., Lampen, A., 2019. Uptake and effects of orally ingested polystyrene microplastic particles in vitro and in vivo. Arch. Toxicol. 93, 1817–1833. https://doi.org/10.1007/s00204-019-02478-7.

Stock, V., Laurisch, C., Franke, J., Dönmez, M.H., Voss, L., Böhmert, L., Braeuning, A., Sieg, H., 2021. Uptake and cellular effects of PE, PP, PET and PVC microplastic particles. Toxicol. Vitr. 70, 105021 https://doi.org/10.1016/j.tiv.2020.105021.

Susanti, N.K.Y., Mardiastuti, A., Wardiatno, Y., 2020. Microplastics and the impact of plastic on wildlife: a literature review. IOP Conf. Ser. Earth. Environ. Sci. 528, 012013 https://doi.org/10.1088/1755-1315/528/1/012013.

Ugwu, K., Herrera, A., Gómez, M., 2021. Microplastics in marine biota: a review. Mar. Pollut. Bull. 169, 112540 https://doi.org/10.1016/j.marpolbul.2021.112540.

Wagner, S., Reemtsma, T., 2019. Things we know and don't know about nanoplastic in the environment. Nat. Nanotechnol. 14, 300–301. https://doi.org/10.1038/s41565-019-0424-z.

Xanthos, D., Walker, T.R., 2017. International policies to reduce plastic marine pollution from single-use plastics (plastic bags and microbeads): a review. Mar. Pollut. Bull. 118, 17–26. https://doi.org/10.1016/j.marpolbul.2017.02.048.

Yagi, M., Kobayashi, T., Maruyama, Y., Hoshina, S., Masumi, S., Aizawa, I., Uchida, J., Kinoshita, T., Yamawaki, N., Aoshima, T., Morii, Y., Shimizu, K., 2022. Microplastic pollution of commercial fishes from coastal and offshore waters in southwestern Japan. Mar. Pollut. Bull. 174, 113304 https://doi.org/10.1016/j.marpolbul.2021.113304.

Yang, D., Shi, H., Li, L., Li, J., Jabeen, K., Kolandhasamy, P., 2015. Microplastic pollution in table salts from China. Environ. Sci. Technol. 49, 13622–13627. https://doi.org/10.1021/acs.est.5b03163.

Yang, Y., Xie, E., Du, Z., Peng, Z., Han, Z., Li, L., Zhao, R., Qin, Y., Xue, M., Li, F., Hua, K., Yang, X., 2023. Detection of various microplastics in patients undergoing cardiac surgery. Environ. Sci. Technol. 57, 10911–10918. https://doi.org/10.1021/acs.est.2c07179.

Zhang, Y., Kang, S., Allen, S., Allen, D., Gao, T., Sillanpää, M., 2020. Atmospheric microplastics: a review on current status and perspectives. Earth Sci. Rev. 203, 103118 https://doi.org/10.1016/j.earscirev.2020.103118.